Mechanism of Phosphate Transfer by Nucleoside Diphosphate Kinase: X-ray Structures of the Phosphohistidine Intermediate of the Enzymes from *Drosophila* and *Dictyostelium*[†,‡]

S. Moréra,[§] M. Chiadmi,[§] G. LeBras,[§] I. Lascu,[||] and J. Janin*[,§]

Laboratoire de Biologie Structurale, UMR 9920 CNRS-Université Paris-Sud, Bâtiment 34, 1, Avenue de la Terrasse, 91198 Gif-sur-Yvette, France, and Institut de Biochimie et Génétique Cellulaires, CNRS-Université Bordeaux 2, 1, rue Camille Saint-Saëns, 33077 Bordeaux, France

Received March 20, 1995; Revised Manuscript Received May 15, 1995[⊗]

ABSTRACT: Nucleoside diphosphate kinase (NDP kinase) has a ping-pong mechanism with a phosphohistidine intermediate. Crystals of the enzymes from *Dictyostelium discoideum* and from *Drosophila melanogaster* were treated with phosphoramidate, and their X-ray structures were determined at 2.1 and 2.2 Å resolution, respectively. The atomic models, refined to *R* factors below 20%, show no conformation change relative to the free proteins. In both enzymes, the active site histidine was phosphorylated on N_δ, and it was the only site of phosphorylation. The phosphate group interacts with the hydroxyl group of Tyr 56 and with protein-bound water molecules. Its environment is compared with that of phosphohistidines in succinyl-CoA synthetase and in phosphocarrier proteins. The X-ray structures of phosphorylated NDP kinase and of previously determined complexes with nucleoside diphosphates provide a basis for modeling the Michaelis complex with a nucleoside triphosphate, that of the phosphorylated protein with a nucleoside diphosphate, and the transition state of the phosphate transfer reaction in which the γ-phosphate is pentacoordinated.

Nucleoside diphosphate kinase (NDP kinase) is responsible for the phosphorylation of the non-adenine nucleoside diphosphates. It catalyses the exchange of a γ-phosphate between nucleoside tri- and diphosphates via a ping-pong mechanism with a high-energy phosphohistidine intermediate:

$$XTP + E \leftrightarrow XDP + E{-}P$$

$$E{-}P + YDP \leftrightarrow E + YTP$$

$$XTP + YDP \leftrightarrow XDP + YTP$$

NDP kinase binds a donor nucleoside triphosphate (XTP), usually ATP, and transfers its γ-phosphate onto a histidine residue at its active site. After releasing XDP, the phosphorylated enzyme binds a nucleoside diphosphate (YDP), and the reverse reaction produces YTP and the free enzyme. Histidine phosphorylation by ATP is fully reversible with an equilibrium constant of about 0.25 (Lascu et al., 1983), and it is very efficient, the turnover number being above 1000 s^{-1} (Garces & Cleland, 1969; Parks & Agarwal, 1973). Thus, the phosphorylation and the dephosphorylation steps must take less than 1 ms, whereas the phosphorylated form is stable for a few hours in the absence of a nucleoside diphosphate acceptor. The NDP kinase reaction is therefore an excellent illustration of enzymic phosphate transfer, with P−N and P−O bonds being formed or broken, depending on the step considered.

We previously determined the X-ray structure of NDP kinases from the slime mold *Dictyostelium discoideum* at 1.8 Å resolution (Dumas et al., 1992; Moréra et al., 1994a) and from *Drosophila melanogaster* at 2.4 Å resolution (Chiadmi et al., 1993). The *Drosophila* enzyme is the product of the *abnormal wing disc (awd)* developmental gene (Dearolf et al., 1988) and will be called Awd for short, the *Dictyostelium* enzyme being Dd. Awd and Dd are hexamers with D_3 symmetry and molecular masses near 100 kDa. Their subunit sequences of respectively 155 and 153 residues show 60% identity. They have the same characteristic fold, based on a four-stranded antiparallel β-sheet, and the active site histidine on edge strand $\beta 4$. This fold is also found in the bacterial NDP kinase from *Myxococcus xanthus*, which is a tetramer (Williams et al., 1993). It differs from all other phosphokinases and most nucleotide-binding proteins, which are built around a parallel β-sheet. The mode of nucleotide binding is also original (Figure 1). The X-ray structures of complexes of *Dictyostelium* NDP kinase with ADP−Mg^{2+} and with dTDP−Mg^{2+} (Moréra et al., 1994b; Cherfils et al., 1994) show that the ribo- and the deoxyribonucleotide bind at the same site and make very similar interactions irrespective of the nature of the base and sugar moieties.

We now report X-ray structures for the phosphorylated forms of *Dictyostelium* and *Drosophila* NDP kinases at 2.1 and 2.18 Å resolution, respectively. Phosphorylation was achieved by diffusing phosphoramidate in the crystals. In both enzymes, we find that phosphate binds covalently to the N_δ atom of the active site histidine. The X-ray structures therefore represent a real intermediate in catalysis. No other

[†] This work was supported in part by funds from Association pour la Recherche contre le Cancer, Agence Nationale de Recherche contre le SIDA and a stipend to S. M. by IFSBM (Villejuif).

[‡] Coordinates have been deposited at the Brookhaven Protein Data Bank under file names 1NSP and 1NSQ.

* Corresponding author (telephone, 33.1.69 82 34 77; fax, 33.1.69 82 31 29; E-mail, janin@cygne.lbs.cnrs-gif.fr).

[§] Laboratoire de Biologie Structurale.

[||] Institut de Biochimie et Génétique Cellulaires.

[⊗] Abstract published in *Advance ACS Abstracts,* July 15, 1995.

0006-2960/95/0434-11062$09.00/0

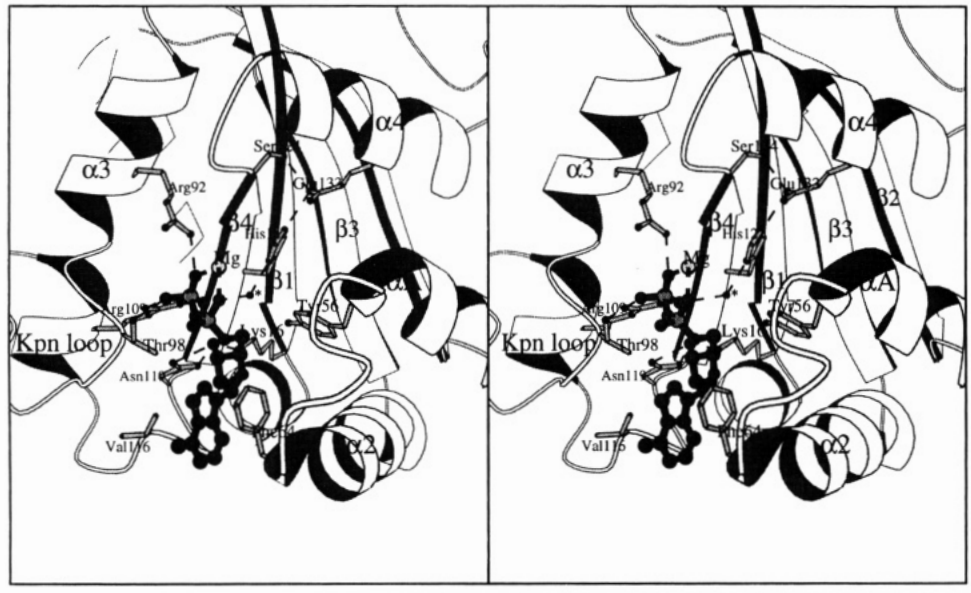

FIGURE 1: Active site of *Dictyostelium* NDP kinase. It shows the characteristic $\beta\alpha\beta\beta\alpha\beta$ topology of the α/β domain (Dumas et al., 1992) in part of subunit B in the ADP−Mg^{2+} complex. The crystal has two subunits in its asymmetric unit and no bound Mg^{2+} in subunit A (Moréra et al., 1994b). The mode of binding shown here is also observed in the dTDP−Mg^{2+} complex (Cherfils et al., 1994), and it is assumed to be the productive mode. All residues interacting with the substrate nucleotide are drawn in ball and stick. The active site His 122 is in the center. ADP−Mg^{2+} (dark bonds) is in a slit formed by helices $\alpha_A-\alpha_2$ on the right and the so-called Kpn loop on the left. Drawn with MolScript (Kraulis, 1991).

residue is phosphorylated, and no conformational change is observed. The environment of the phosphohistidine is compared with that in other proteins where histidine phosphorylation occurs: succinyl-coA synthetase (Wolodko et al., 1994) and the HPr and domain III^{Glc} components of bacterial sugar transport (van Nuland et al., 1995; Pelton et al., 1992). The X-ray structures of phosphorylated NDP kinase and the nucleoside diphosphate complexes provide a basis for modeling (a) the Michaelis complexes for the two steps of the reaction, the free enzyme with ATP and the phosphorylated enzyme with ADP, and (b) the putative transition state for in-line phosphate transfer in which the P_γ atom of ATP is pentacoordinated and bound to both the β-phosphate and His 122. The modeling confirms and extends a catalytic mechanism proposed by Moréra et al. (1994b) and tested by site-directed mutagenesis (Tepper et al., 1994). The proposed catalytic mechanism of NDP kinase is relevant to enzymic catalysis of phosphate transfer in general.

MATERIALS AND METHODS

Protein Preparation, Crystallization, and Data Collection. The cloned *gip17* gene from *D. discoideum* (Lacombe et al., 1990) was expressed in *Escherichia coli*, and active NDP kinase was purified as described in Wallet et al. (1990). Crystallization was performed in hanging drops containing 5% PEG 6000 (Sigma), 20 mM $MgCl_2$, and 50 mM Tris-HCl buffer, pH 8.0, over pits containing 10% PEG 6000 in the same buffer. The crystals grew in a few days at 18 °C. They were identical to those reported in Moréra et al. (1994a) and belong to the hexagonal space group $P6_322$ with one 17 kDa subunit in the asymmetric unit. To prepare the phosphorylated protein, crystals were soaked with 40 mM phosphoramidate during 1 h before data collection with no apparent damage or change in cell parameters. The synthesis of dipotassium phosphoramidate was performed by the method of Wei and Matthews (1991).

The *awd* gene from *D. melanogaster* cloned into a pET3C expression vector (Timmons et al., 1993) was expressed in *E. coli*. Purification used a DEAE ion-exchange resin to separate the basic Awd protein from the bulk of acidic *E. coli* proteins, followed by affinity chromatography on a Blue Sepharose column and elution with a buffer containing ATP. Crystals of the recombinant protein grew in ammonium sulfate, under the same conditions as for the protein prepared from *Drosophila* flies that was used in Chiadmi et al. (1993). They belong to trigonal space group $P3_221$ and have a 50 kDa trimer in their asymmetric unit. Crystals were soaked for 3 h in 200 mM phosphoramidate before data collection with no apparent damage or change in cell parameters.

X-ray diffraction data were collected at the W32 station in the LURE-DCI synchrotron radiation center (Orsay, France), using only one crystal soaked in phosphoramidate for each structure. The crystals were kept at 4 °C during data collection. The station was equiped with a MAR-research photosensitive image plate system, and the monochromator was set to a wavelength of 0.9 Å. For the *Dictyostelium* crystal, we recorded 60 deg of rotation about the *c* axis at a rate of 1.5 deg per 90 s exposure and per image. With the Awd crystal, 60 deg of rotation were collected at a rate of 1 deg per 240 s and per image. Intensities were evaluated with program MOSFLM as adapted for the image plate system (Leslie et al., 1986). Further processing used the CCP4 program suite (CCP4, 1979). Statistics are reported in Table 1.

Structure Solution and Refinement. Crystallographic refinement of the phosphorylated Dd structure was performed with the conjugate-gradient facility of X-PLOR (Brünger et al., 1987). The starting point was a refined model of wild-type *Dictyostelium* NDP kinase at 1.8 Å resolution (Moréra et al., 1994a). The initial *R* factor against the new data was 0.26 at 2.5 Å resolution. It dropped to 0.22 after 100 cycles of Powell minimization. An electron density map calculated with phases from the refined model showed density in the

Table 1: Statistics on Crystallographic Analysis

NDP kinase	*Dictyostelium* Dd	*Drosophila* Awd
diffraction data		
space group	$P6_322$	$P3_221$
cell parameters $a = b$, c (Å)	75.16, 105.93	115.75, 98.52
resolution (Å)	2.1	2.18
measured intensities	74522	184822
unique reflections	10810	32198
completeness (%)	97	79
R_{merge} (%)[a]	4.5	7.7
refinement		
R_{cryst} (%)[b]	18.8	18
reflections	10663	31522
protein atoms	1152	3621
solvent atoms	82	244
average B (Å^2)	26.8	22.0
geometry[c]		
bond distances (Å)	0.014	0.010
bond angle (deg)	1.67	1.59
peptide ω angle (deg)	1.64	1.27

[a] $R_{merge} = \sum_{hi}|I(h)_i - \langle I(h)\rangle|/\sum_{hi}I(h)_i$. [b] $R_{cryst} = \sum_h||F_o| - |F_c||/\sum_h|F_o|$ calculated with X-PLOR on all reflections with $F > 2\sigma$. [c] Root-mean-square deviations from ideal values.

vicinity of the His 122 side chain. A phosphohistidine model was built with parameters from model compound IMZPHZ (Ritchie et al., 1980) taken from the Cambridge Structural Data Bank. Refinement was continued at progressively increasing resolution until an R factor of 0.188 at the 2.1 Å resolution limit was reached. Weak reflections (F less than 2σ), which were excluded from refinement, represent only 0.9% of the data. $2F_o - F_c$ and $F_o - F_c$ electron density maps with calculated phases were examined with FRODO (Jones, 1985) at various steps to make necessary corrections and add or remove water molecules.

Refinement of the phosphorylated Awd structure was carried out with PROLSQ (Hendrickson, 1985) starting with the atomic model of *Drosophila* NDP kinase (Chiadmi et al., 1993). After 30 cycles of individual atomic refinement with PROLSQ against the data collected for the phosphorylated protein, the model had an R factor of 0.25 at 2.2 Å resolution. In each of the three subunits of the asymmetric unit, a $2F_o - F_c$ map showed additional density close to the active site His 119 (Awd numbering) in which phosphohistidine was then modeled with FRODO (Jones, 1985). PROLSQ refinement was then continued until the R factor reached 0.19. Statistics given in Table 1 are derived by running X-PLOR on the final model for consistency with data on Dd.

Reliability of the Models. Both final models have an R factor below 20% against essentially all data and good stereochemistry (Table 1). The Dd model contains 1152 protein atoms corresponding to residues 6−155 of the NDP kinase subunit including the phosphate on His 122 and 82 water molecules. The N-terminal Met 1 is absent in the protein expressed in *E. coli*, and like in other X-ray structures of the protein, no electron density is seen for residues 2−5. The density is otherwise well-defined everywhere except for the side chains of residues 57−64 in a loop connecting helices α_A and α_2 and of residues 139−151 in the C-terminal segment. These regions have larger than average temperature factors in the phosphorylated as in the free protein.

The final model of the Awd structure contains 1207 atoms in each of the three subunits (called A, B, and C for convenience) and 244 water molecules in total. Each chain has 153 residues missing the N-terminal Met 1 and including the phosphohistidine. The electron density is well-defined everywhere except for residue 2 of the B chain. A pairwise C_α superposition of the three chains led to rms differences of 0.31, 0.32, and 0.40 Å. These values are similar to those observed before phosphorylation, and they provide an upper estimate of the error on atomic coordinates.

RESULTS AND DISCUSSION

The Phosphohistidine at the Active Site. NDP kinase phosphorylation by its natural substrate, ATP, was not possible in the crystals. Attempts to diffuse ATP (or other nucleotides) in hexagonal crystals of the *Dictyostelium* enzyme failed as crystal packing blocks the site that the base occupies in the ADP or dTDP complexes (Moréra et al., 1994a). These complexes had to be analyzed in different crystal forms after cocrystallization (Moréra et al., 1994b; Cherfils et al., 1994). The rate of hydrolysis of phosphorylated NDP kinase is slow enough for X-ray data collection with synchrotron radiation but not for cocrystallization. Thus, we looked for nonnucleotide phosphorylating compounds that could be diffused in the hexagonal crystals and reach the active site in spite of the crystal packing. If they phosphorylate the active site histidine, albeit slowly, they should be substrates of NDP kinase. Phosphoramidate ($NH_2PO_3^{2-}$) was chosen because it is much more reactive toward nitrogen than oxygen nucleophiles (Benkovic & Sampson, 1971) and it phosphorylates histidine (Gassner et al., 1977). It has been reported to be the substrate of a phosphotransferase that can make ADP into ATP (Dowler & Nakada, 1967) and may therefore well be a NDP kinase. We find phosphoramidate to be a very poor substrate of *Dictyostelium* NDP kinase, with a turnover number less than 1 h^{-1}, but the protein modified by phosphoramidate can transfer a phosphate to a nucleoside diphosphate (data not shown).

Phosphoramidate being suitable for crystallographic experiments, we used it with both the *Dictyostelium* and *Drosophila* enzymes. The two X-ray structures actually provide four crystallographically independent images of the phosphorylated protein: one in Dd and three in subunits A, B, and C of Awd. The active site histidine is His 122 in Dd and His 119 in Awd. Since residues near the active site are conserved in the two enzymes (and in other NDP kinase sequences), the Dd numbering will be used below for both. In the phosphorylated Dd structure, the phosphate moiety attached to His 122 had clear density, but its oxygen atoms were ill defined and their mean temperature factor became much higher than for surrounding protein atoms if refinement was performed with 100% occupancy of the phosphate group. Its occupancy was therefore set to 50%. In Awd, the phosphate density showed more details of the oxygen positions (Figure 2), and the temperature factors were compatible with a higher degree of modification of the active site histidine. Full occupancy was therefore assumed. The difference can be attributed to the lower phosphoramidate concentration and shorter soaking time used when collecting data on the Dd crystal.

In both enzymes, phosphorylation was observed to occur exclusively on the active site histidine. Phosphorylation of other histidine residues or of Ser 124, which is adjacent to His 122 on strand β4, could not be detected in the electron density. The modification had no effect on the protein

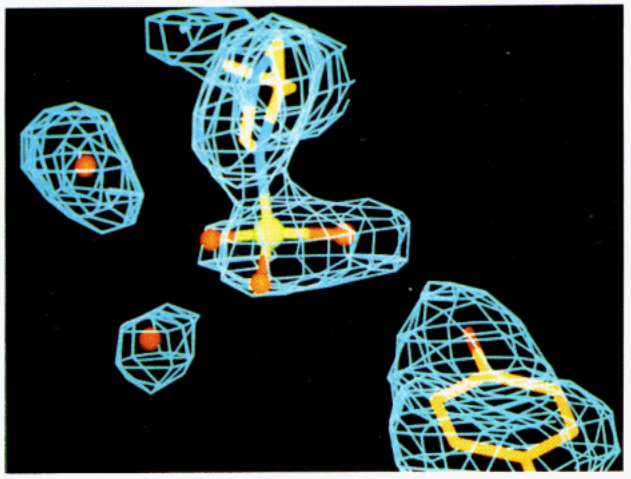

FIGURE 2: Final electron density map. $2F_o - F_c$ map contoured at 1.2σ around the phosphohistidine, Tyr 56, and two interacting water molecules in subunit A of *Drosophila* NDP kinase. Drawn with program O (Jones et al., 1991).

structure either at the level of the hexamer or within the subunit. For both *Dictyostelium* and *Drosophila* NDP kinases, a superposition of C_α positions in the free and phosphorylated enzymes gave a RMS deviation of 0.16 Å, less than the estimated error on atomic positions. The RMS deviation was 0.33 Å for all Dd atoms and 0.40 Å for all Awd atoms. At the active site, very little change could be observed beyond the presence of the phosphate group, the displacements of several solvent molecules, and small movements of the Arg 92 side chain.

The geometry of the phosphohistidine is described in Table 2 and Figure 3. It is essentially the same at all four active sites. The conformation of His 122 is unchanged from the free enzyme as indicated by the χ_1 and χ_2 angles, and its imidazole group is held in position by the hydrogen bond from the N_ϵ atom to Glu 133 as in the free enzyme. The orientation of the phosphate is defined by χ_3 in Table 2. One oxygen interacts with the hydroxyl group of Tyr 56. Other polar interactions are made through water molecules bridging phosphate oxygens to the side chains of Arg 92 and Asn 119 and to the backbone NH of Gly 123. The ϵ-amino group of Lys 16 is 3.6−3.9 Å and the guanidinium group of Arg 109 is 4.2−4.6 Å from the phosphate oxygens. This precludes a direct electrostatic interaction, but in Awd at least, water-mediated interactions are also observed with these residues.

The phosphorus atom refines to a position slightly out of the plane of the imidazole ring. The mean of four distances to the plane is 0.27 Å, and the P−N bonds make an angle of 9 deg with the plane of the ring. Though these values border the limit of the accuracy of the model, their consistency and the shape of electron density in Figure 2 suggest that the distortion is real. It displaces the phosphate group toward Tyr 56 and could be attributed to the interaction with this residue.

Comparison with Phosphohistidines in Other Proteins. Histidine phosphorylation occurs in several cellular and biochemical contexts. In addition to NDP kinase, structural data are available for a number of enzymes—phosphoglycerate mutase (Campbell et al., 1974), succinyl-CoA synthetase (Wolodko et al., 1994), and acid phosphatase (Schneider et al., 1993)— and for protein components of signaling pathways and sugar transport in bacteria— HPr (Wittekind et al., 1990; Herzberg et al., 1992), domain IIA of glucose permease (Liao et al., 1991; Hurley et al., 1993), and protein III^{Glc} (Worthylake et al., 1991). With few exceptions, the structural data refer to the free rather than the phosphorylated forms. The exceptions are succinyl-CoA synthetase, HPr, and III^{Glc}, the last two being NMR structures (van Nuland et al., 1995; Pelton et al., 1992).

Succinyl-CoA synthetase catalyzes the phosphorylation of succinate by ATP via a phosphohistidine intermediate, followed by transfer of the succinyl moiety onto coenzyme A. The first part of the reaction is a transfer of the γ-phosphate of ATP onto a histidine, just as in NDP kinase. The two enzymes bear no structural relationship, *E. coli* succinyl-CoA synthetase is an $\alpha_2\beta_2$ heterotetramer, and the active site His α246 was phosphorylated by ATP before crystallization. This implies that the phosphohistidine has an abnormal high stability due to the protein environment. The X-ray structure shows that it is located at the interface between α and β subunits and that the phosphate moiety interacts with the N-terminus of two α-helices, the dipole moment of which may contribute to stabilization (Wolodko et al., 1994). The phosphate is on the N_ϵ atom of the imidazole group, and its N_δ atom hydrogen bonds to a glutamate side chain. The latter interaction appears to be the only common feature with NDP kinase, where the phosphohistidine is not at a subunit interface and does not interact with α-helices, and there is no indication that it is stabilized by the protein environment. The equilibrium constant with ATP is not far from unity and spontaneous hydrolysis has approximately the same half-life in the native or the denatured protein (Bominaar et al., 1994; Lecroisey et al., 1995).

In the histidine phosphocarrier protein HPr, the active site His 15 receives its phosphate from one component of the bacterial sugar transport system and transfers it to another. Phosphorylation cannot be performed in the crystal, but NMR data are available on the phosphorylated protein (van Nuland et al., 1995). HPr is comparable in size to the NDP kinase subunit, and both are built around a four-stranded antiparallel β-sheet, albeit with a different topology (Swindells et al., 1993; Janin, 1993; Liao & Herzberg, 1994). His 15 in HPr is at the N-terminus of an α-helix, and its phosphate moiety interacts with the backbone amide of residues in the first helix turn. These interactions have no counterpart in NDP kinase, where the phosphohistidine is part of a β-strand and the only direct phosphate−protein interaction is to a tyrosine hydroxyl group.

NDP Kinase Catalysis Involves Little Induced Fit and No High-Energy Conformation. The structure of phosphorylated Dd and Awd NDP kinases is remarkably similar to that of the free enzymes. No conformation change is observed, even at the active site. The free and phosphorylated forms represent two stages in the catalytic pathway. In between, there is the binding of a nucleoside triphosphate and the release of a diphosphate. Nucleotide binding is accompanied with a small, but detectable, conformational change in the protein. In both the ADP and the dTDP complexes with Dd, the base and sugar fit in a slit between the pair of helices $\alpha_A-\alpha_2$ and the main body of the protein (Figure 1). Helices $\alpha_A-\alpha_2$ are on the protein surface, and they move together by 1−2 Å to lock the substrate nucleotide in the slit. Presumably, the reverse movement is required to let it in or out.

Table 2: Conformation and Interactions of the Phosphohistidine

	Dictyostelium Dd[a]		*Drosophila* Awd[b]	
	free	phosphorylated	free	phosphorylated
dihedral angles (deg)[c]				
χ_1	161	168	164 (3)	165 (4)
χ_2	88	86	84 (4)	90 (2)
χ_3		160		172 (7)
planarity				
P_γ to plane (Å)		0.24		0.28 (0.08)
hydrogen bond distances (Å)				
N_ϵ–Glu 133 ($O_{\epsilon 2}$)	2.7	3.0	3.0 (0.2)	2.9 (0.1)
O_1–Tyr 56 (O_η)		2.8		2.8 (0.2)
O_3–Wat 1		2.9		2.9 (0.1)
O_3–Wat 2		3.2		2.7 (0.1)

[a] His 122. [b] His 119. Mean and (in parentheses) RMS deviation in subunits A, B, and C of the asymmetric unit. [c] χ_3 is the C_γ–N_δ–P–O_2 dihedral angle of rotation about the P–N bond, O_2 being the phosphate oxygen closest to the plane of the imidazole.

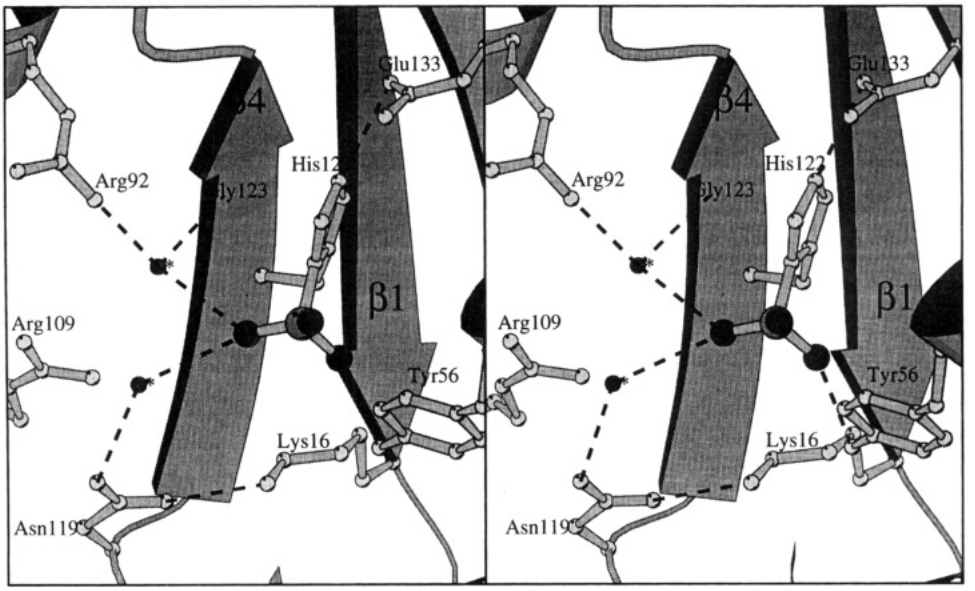

FIGURE 3: Phosphohistidine and its environment in the X-ray structure of *Dictyostelium* NDP kinase. The phosphate group hydrogen bonds to Tyr 56 and two water molecules (dashed lines). The orientation is approximately the same as in Figure 1. Drawn with MolScript (Kraulis, 1991).

The movement of helices α_A–α_2 may be interpreted as an example of induced fit (Koshland, 1958), a rather general feature of ATP-dependent phosphokinases. It is a very poor example when compared to other enzymes of this family. The amplitude of the movement is much less than, for instance, in adenylate kinase (Schulz et al., 1990) or hexokinase (Bennett & Steitz, 1980). Hexokinase transfers the γ-phosphate of ATP onto a hydroxyl group. It must shield its catalytic center from water unless it becomes an ATPase (Jencks, 1975). It achieves this goal by a large movement involving whole domains of the protein. Also, a base is required for activating the hydroxyl group and taking its proton away before forming the P–O bond (Knowles, 1980). The same base could activate water if present. In NDP kinase, there appears to be no catalytic base, and there is no need for one as long as the target N atom is unprotonated. At pH's where the enzyme is active, the His 122 imidazole carries only one acidic proton which is kept on N_ϵ by the bond to Glu 133, leaving N_δ free to react. Presumably, this remark also applies to succinyl-CoA synthetase after exchanging N_δ and N_ϵ.

NDP kinase has a single residue with an unfavorable backbone conformation. Ile 120, part of a γ-turn just preceding strand β_4 and very close to the active site, has a positive ϕ angle in the X-ray structures of *Dictyostelium*, *Drosophila*, and *Myxococcus* NDP kinases. One could imagine that this conserved peculiarity is part of the catalytic mechanism. Releasing strain in the main chain via a local conformation change occurring during phosphate transfer would lower the transition-state energy and accelerate the reaction. The X-ray structure of *Streptococcus faecalis* HPr also shows an abnormal main-chain conformation near the active site histidine, and it has been proposed that it is relaxed upon phosphorylation (Jia et al., 1993). Other HPr structures strongly argue against this hypothesis (Liao & Herzberg, 1994; van Nuland et al., 1995). In protein III^{Glc}, histidine phosphorylation has little effect on the protein structure (Pelton et al., 1992). In NDP kinase, we find the phosphorylated protein to have exactly the same conformation at Ile 120 as in either the free enzyme or the complexes with nucleoside diphosphates. It is therefore unlikely to change during phosphate transfer. Moreover, *E. coli* NDP kinase appears to have a glycine at the equivalent position, and the I120G mutant of *Dictyostelium* NDP kinase is enzymatically active (A. D. Tepper and M. Véron, personal communication). The glycine substitution should relieve strain in the main chain associated with the positive ϕ angle.

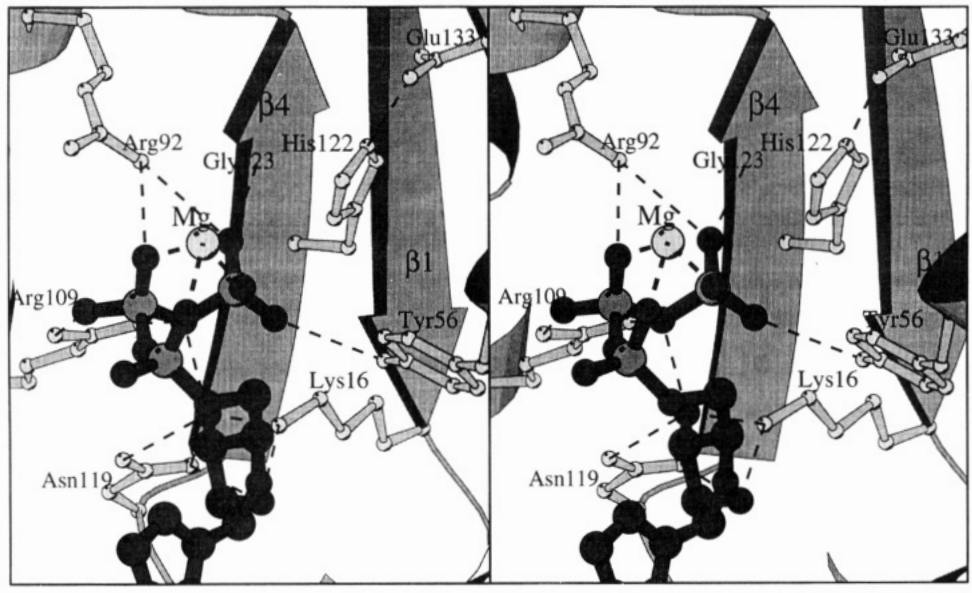

FIGURE 4: : Model-built Michaelis complex with ATP. The model was built by adding a γ-phosphate to ADP in subunit B of the X-ray structure described by Moréra et al. (1994b). The Mg^{2+} ion has been moved by about 1 Å to form a bond with the added phosphate group. Otherwise, only water molecules have been displaced. The figure is oriented approximately as in Figure 1, with the six-membered ring of the adenine base missing at the bottom edge of the drawing. Drawn with MolScript (Kraulis, 1991).

Modeling Phosphate Transfer in NDP Kinase. Taken together with those of the ADP and dTDP complexes, the X-ray structure of phosphorylated NDP kinase provides a detailed picture of catalysis. The complexes of the non-phosphorylated enzyme with nucleoside diphosphates are not productive, but they may be used in building models for the two productive complexes of the free enzyme with ATP and of the phosphorylated enzyme with ADP. Figure 4 shows a model of the first complex for the *Dictyostelium* enzyme. In this model, the ADP moiety of ATP occupies the same position as in subunit B of the ADP complex (where the two subunits of the crystal asymmetric unit show slightly different modes of nucleotide binding, subunit A having no bound Mg^{2+}). The γ-phosphate finds a location near His 122, with P_γ at about 3.2 Å of N_δ. Two of the phosphate oxygens interact with the backbone NH of Gly 123, the Arg 92 guanidinium group, and the Tyr 56 hydroxyl. They replace water molecules that make the same interactions in the X-ray structures. The third oxygen is in position to bind the Mg^{2+} ion, which now bridges all three phosphate groups of ATP with metal−oxygen bonds in the 2.1−2.5 Å range. In the dTDP complex and in subunit B of the ADP complex, Mg^{2+} shows octahedral coordination to two oxygen ligands from the α- and β-phosphates and four from water molecules. One of the waters is now replaced by the γ-phosphate oxygen.

NDP kinase shows high stereospecificity for the *S* diastereomer of ATPαS and the *R* diastereomer of ATPβS where the sulfur atom on the α- or β-phosphate makes it chiral (Eckstein & Goody, 1976; Cohn, 1982). Considering that the Mg^{2+} ion should have a higher affinity for an oxygen than a sulfur ligand, this result is compatible with the location of the metal relative to the phosphate groups in our model. In addition, the γ-phosphate is approximately at one of two alternative positions occupied by the β-phosphate of ADP complexed to *Myxococcus* NDP kinase (Williams et al., 1993).

The model can be taken one step further into the transition state for in-line phosphate transfer which is depicted in Figure 5. There, the γ-phosphate is placed halfway between the β-phosphate and the side chain of His 122, with the phosphorus atom at the location occupied by a bridging water molecule in the complex with ADP (Moréra et al., 1994b). The P_γ atom has moved by about 1 Å from its location in the Michaelis complex above. P_β is still in the same position. A χ_2 rotation in His 122 and a rotation around the $P_\alpha-O-P_\beta$ anhydride bonds are the only changes needed in order to bring P_γ on a line with O_7 and N_δ of His 122. The movement is accompanied with a change from a tetrahedral to a trigonal-bipyramidal geometry as P_γ forms a fifth bond to the N_δ of His 122. In the pentacoordinated transition-state intermediate, the two apical $P_\gamma-O_7$ and $P_\gamma-N_\delta$ bonds should be longer than the equatorial bonds. In the model, they are 2.1−2.2 Å long rather than the usual 1.5−1.7 Å. The geometry is the one expected for the in-line associative mechanism of transfer (Knowles, 1980).

In Figure 6, the transition state is compared with a model of the ADP complex with the phosphorylated protein which is the Michaelis complex for the second step of the NDP kinase reaction. This model was obtained by combining the two X-ray structures of the phosphorylated protein and of the ADP complex. Relative to the transition state, the His 122 side chain is seen to have rotated about the $C_\beta-C_\gamma$ bond by about 30° and the phosphorus atom to have moved by about 2 Å. Otherwise, very little has changed.

Structural Elements Involved in Catalysis. In the transition state, the imidazole group acquires a positive charge while an additional negative charge develops on the equatorial oxygens. These oxygens maintain the bond to Mg^{2+} and the hydrogen bonds to Arg 92, Tyr 56, and the NH of Gly 123 which were described for the Michaelis complex. Charge separation in the transition state could be avoided by a simultaneous proton transfer from Tyr 56 to the γ-phosphate and from N_ϵ of His 122 to Glu 133. Results of site-directed mutagenesis studies argue against such proton transfers. Mutants of *Dictyosytelium* NDP kinase where Glu 133 is substituted with Asp or Gln have residual activity (Tepper

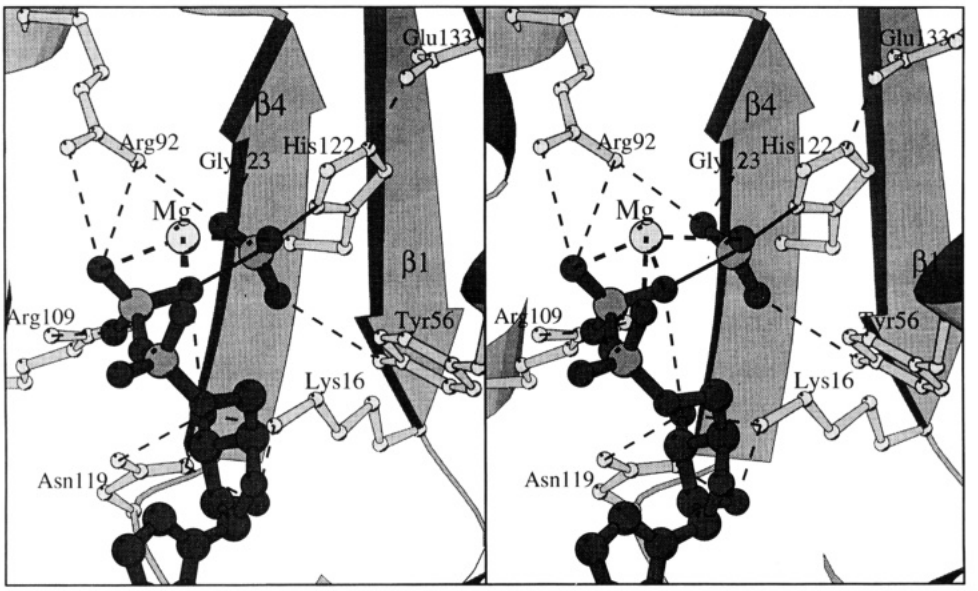

FIGURE 5: Model-built transition state for in-line phosphate transfer between ATP and His 122. The γ-phosphate adopts a trigonal-bipyramidal geometry. The three oxygens in the equatorial plane carry a negative charge which is compensated in part by Arg 92 and the Mg^{2+} ion. Solid lines represent the partial bonds made to the β-phosphate and to N_δ of His 122; dashes, hydrogen bonds or metal−oxygen bonds. The figure is oriented as in Figure 4. Drawn with MolScript (Kraulis, 1991).

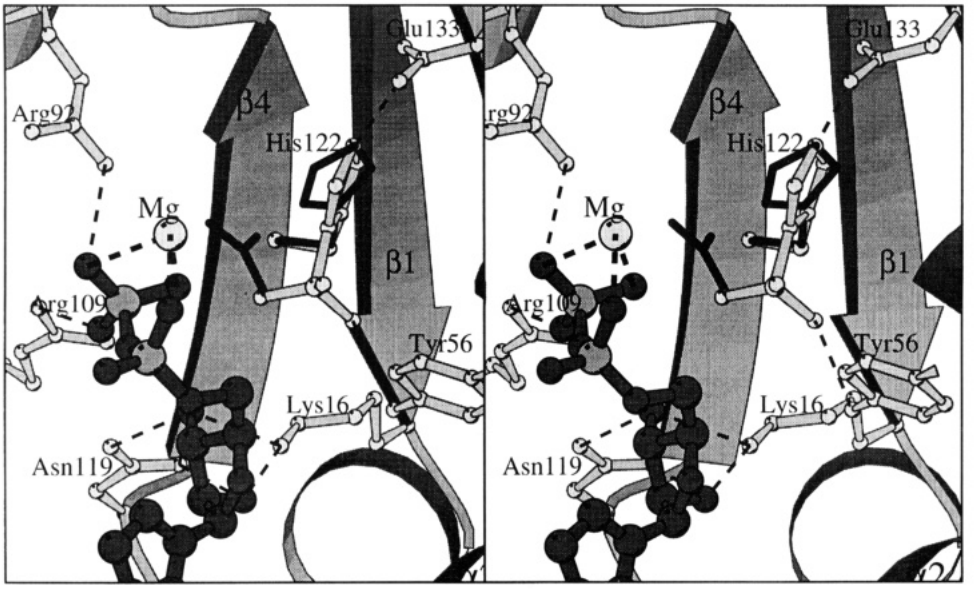

FIGURE 6: Model-built Michaelis complex of phosphorylated NDP kinase with ADP. The nucleotide has the same position and conformation as in Figure 5. The γ-phosphate has left its position in the transition state (dark lines) to form a covalent bond with His 122. A 30° rotation of the imidazole group is needed to achieve the conformation seen in crystals of the phosphorylated protein (light bonds). The same rotation also relieves close contacts between phosphate oxygen atoms. The figure is oriented as in Figures 4 and 5. Drawn with MolScript (Kraulis, 1991).

et al., 1994). It reaches 0.5% in the case of a glutamine, the amide group of which can hydrogen bond to N_ϵ of His 122 just as Glu 133 does but cannot take its proton away. Mutants where Tyr 56 has been replaced with either Phe or Ala retain 2% of wild-type activity. Rather than supporting a role in acid catalysis, the remaining activity suggests that the hydroxyl group of Tyr 56 contributes of the order of $-RT \ln 0.02 = 2.3$ kcal mol^{-1} to stabilizing the transition state relative to the Michaelis complex. It hydrogen bonds to the γ-phosphate in both Figure 4 and Figure 5 as it does with the phosphohistidine product in Figure 3. The hydroxyl group may then be given the same role as the oxyanion hole in serine proteases: in the transition state, the hydrogen bond acceptor is an oxyanion making the bond stronger than to the substrate phosphate oxygen which carries only a partial negative charge.

Other charged residues which could interact with the equatorial oxygens in the transition state are Arg 92, Arg 109, and Lys 16. Replacing Arg 92 or Arg 109 with an alanine leaves less than 1% of the activity whereas the replacement with a lysine leaves 5−10%. This fits with the role of Arg 92 in neutralizing charges on the γ-phosphate and of Arg 109 in doing the same on the β-phosphate which is the leaving group of the reaction. In the free enzyme, Arg 109 is held in position by hydrogen bonds to the main chain. In contrast, the Arg 92 side chain is free to move, and it can follow the movement of the γ-phosphate throughout the reaction. The case of Lys 16 is more complex. In

all NDP kinase X-ray structures, its ϵ-amino group hydrogen bonds with the side chain of Asn 119. Data on Lys 16 and Asn 119 mutants suggest that this bond is important to the stability of the protein (Tepper et al., 1994). In complexes with ADP or dTDP, both Asn 119 and Lys 16 interact with the sugar hydroxyl rather than with the phosphates. Their contribution to substrate binding is a sufficient explanation for the low residual activity of the mutants (less than 1%), but that does not exclude a role of Lys 16 in catalysis. In the modeled ATP complex and transition state, its ϵ-amino group can easily be made to interact with the γ-phosphate after breaking the hydrogen bonds to Asn 119 and to the sugar hydroxyls. In Figures 4 and 5, the latter interactions are retained and the ϵ-amino group is about 3.5 Å of the nearest γ-phosphate oxygen, a distance which could be made shorter by small displacements of the two partners. Lys 16 is certainly an important residue in NDP kinase, but an exact definition of its role will require more biochemical data.

The model also implicates two nonprotein components in the reaction mechanism. One is the Mg^{2+} ion, which neutralizes charges on the β- and γ-phosphates. Its plays an essential role in catalysis by NDP kinase as with other ATP- (or GTP-) dependent phosphotransferases (Villafranca & Nowak, 1992) and in nonenzymic phosphate transfer (Herschlag & Jencks, 1990). NDP kinase phosphorylation can been observed in the absence of added divalent ions (Munoz-Dorado et al., 1993), but it may take seconds or minutes. In the presence of Mg^{2+}, it takes less than 1 ms, being part of a catalytic cycle with a turnover number above 1000 s^{-1}. The other component is the 3′-hydroxyl on the nucleotide sugar. In the ADP and dTDP complexes, it donates a hydrogen bond to the β-phosphate. In the modeled complexes, it can do the same to the γ-phosphate, and therefore, it might be given a similar role to Tyr 56. The 3′-hydroxyl of the ribo- and the deoxyribonucleotides is missing in the dideoxy analogues which are very poor substrates of NDP kinase (I. Lascu and M. Véron, private communication).

Conclusion. The catalytic mechanism of phosphate transfer has often been the subject of much discussion (Frey, 1992) even in systems such as ribonuclease A, adenylate kinase, or the $p21^{ras}$ GTPase where structural and biochemical data are abundant. In comparison, NDP kinase has some very favorable features. The phosphorylated form is a true intermediate of the reaction that is reasonably stable and can be subjected to structural studies by X-rays or ^{31}P NMR (Lecroisey et al., 1995). The catalytic cycle requires no major conformation change in either the enzyme or the substrate. As a consequence, X-ray structures and biochemical data give a rather clear picture of each step. The present mechanism is based on data obtained mostly with the *Dictyostelium* and *Drosophila* enzymes. It certainly applies to all other NDP kinases, since the active site residues are strictly conserved. We expect that several of its features will be shared by other phosphate transfer enzymes and especially by those which catalyze P−N bond formation.

ACKNOWLEDGMENT

We thank Dr. M. Véron, A. Lecroisey, and M. Delepierre (Institut Pasteur, Paris) for discussion. We are grateful to Dr. A. Shearn (Johns Hopkins University, Baltimore) for the gift of the *awd* expression plasmid, to R. Warth for help in preparing the Awd protein, to Pr. R. Fourme, Pr. J. P. Benoît, and the staff of LURE (Orsay) for making station W32 on the wiggler line of LURE-DCI available to us, to Dr. L. Tchertanov and B. Arnoux (Gif-sur-Yvette) for references in the Cambridge Structural Data Base, and to Dr. M. E. Fraser and M. N. G. James (Edmonton, Alberta) for atomic coordinates of succinyl-CoA synthetase.

REFERENCES

Benkovic, S. J., & Sampson, E. J. (1971) *J. Am. Chem. Soc. 93,* 4009−4016.

Bennett, W. S., Jr. & Steitz, T. A. (1980) *J. Mol. Biol. 140,* 211−230.

Bominaar, A. A., Tepper, A. D., & Véron, M. (1994) *FEBS Lett. 353,* 5−8.

Brünger, A. T., Kuriyan, J., & Karplus, M. (1987) *Science 235,* 458−460.

Campbell, J. W., Watson, H. C., & Hodgson, G. I. (1974). *Nature, 250,* 301−303.

CCP4 (1979) Collaborative Computational Project No. 4 on Protein Crystallography, SERC, Daresbury, Warrington, U.K.

Cherfils, J., Moréra, S., Lascu., I., Véron, M., & Janin, J. (1994) *Biochemistry 33,* 9061−9069.

Chiadmi, M., Moréra, S., Lascu, I., Dumas, C., Le Bras, G., Véron, M., & Janin, J. (1993) *Structure 1,* 283−293.

Cohn, M. (1982) *Acc. Chem. Res, 15,* 326−332.

Dearolf, C. R., Tripoulas, N., Biggs, J., & Shearn, A. (1988) *Dev. Biol. 129,* 169−178.

Dowler, M. J., & Nakada, H. I. (1967) *J. Biol. Chem. 243,* 1434−1440.

Dumas, C., Lascu, I., Moréra, S., Glaser, P., Fourme, R., Wallet, V., Lacombe, M.-L., Véron, M., & Janin, J. (1992) *EMBO J. 11,* 3203−3208.

Eckstein, F., & Goody, R. S. (1976) *Biochemistry 15,* 1685−1691.

Frey, P. A. (1992) *Enzymes, 3rd Ed. 20,* 142−186.

Garces, E., & Cleland, W. W. (1969) *Biochemistry 8,* 633−640.

Gassner, M., Stehlick, D., Schrecker, O., Hengstenberg, W., Maurer, W., & Rüterjans, H. (1977) *Eur. J. Biochem. 75,* 287−296.

Hendrickson, W. A. (1985) *Methods Enzymol. 115,* 252−271.

Herschlag, D., & Jencks, W. P. (1990) *J. Am. Chem. Soc. 112,* 1942−1950.

Herzberg, O., Reddy, P., Sutrina, S., Saier, M. H., Jr., Reizer, J., & Kapadia, G. (1992) *Proc. Natl. Acad. Sci. U.S.A. 89,* 2499−2503.

Hurley, J. H., Faber, H. R., Worthylake, D., Meadow, N. D., Roseman, S., Pettigrew, D. W., & Remington, S. J. (1993) *Science 289,* 673−677.

Janin, J. (1993) *Nature 365,* 21.

Jencks, W. P. (1975) *Adv. Enzymol. 43,* 219−410.

Jia, Z., Vandonselaar, M., Quail, W., & Delbaere, L. T. J. (1993) *Nature 361,* 94−97.

Jones, T. A. (1985) *Methods Enzymol., 115,* 157−171.

Jones, T. A., Zou, J.-Y. , Cowan, S. W., & Kjeldgaard, M. (1991) *Acta Crystallogr. A47,* 110−119.

Knowles, J. R. (1980) *Annu. Rev. Biochem. 49,* 877−919.

Koshland, D. E. (1958) *Proc. Natl. Acad. Sci. U.S.A. 44,* 98.

Kraulis, P. J. (1991) *J. Appl. Crystallogr. 24,* 946−950.

Lacombe, M. L., Wallet, V., Troll, H., & Véron, M. (1990) *J. Biol. Chem. 17,* 10012−10018.

Lascu, I., Pop, R. D., Porumb, H., Presecan, E., & Proinov, I. (1983) *Eur. J. Biochem. 135,* 497−503.

Lecroisey, A., Lascu, I., Véron, M., & Delepierre, M. (1995) *Biochemistry* (submitted for publication).

Leslie, A. G. W., Brick, P., & Wonacott, A. T. (1986) *CCP4 Daresbury Lab. Inf. Q. Protein Crystallogr., 18,* 33−39.

Liao, D. I., & Herzberg, O. (1994) *Structure 2,* 1203−1216.

Liao, D. I., Kapadia, G., Reddy, P., Saier, M. H., Jr., Reizer, J., & Herzberg, O. (1991) *Biochemistry 30,* 9583−9594.

Moréra, S., Le Bras, G., Lascu, I., Lacombe, M. L., Véron, M. & Janin, J. (1994a) *J. Mol. Biol. 243,* 873−890.

Moréra, S., Lascu, I., Dumas, C., Le Bras, G., Briozzo, P., Véron, M., & Janin J. (1994b) *Biochemistry 33*, 459−467.
Munoz-Dorado, J., Almaula, N., Inouye, S., & Inouye, M. (1993) *J. Bacteriol. 175*, 1176−1181.
Parks, R. E., Jr., & Agarwal, R. P. (1973) in *The Enzymes* (Boyer, P. D., Ed.) Vol. 8, pp 307−334, Academic Press, New York.
Pelton, J. G., Torchia, D. A., Meadow, N. D., & Roseman, S. (1992) *Biochemistry 31,* 5215−5224.
Ritchie, R. J., Fuller, T. J., & Allcock, H. R. (1980) *Inorg. Chem. 19*, 3842.
Schneider, G., Lindqvist, Y., & Vihko, P. (1993) *EMBO J. 12*, 2609−2615.
Schulz, G. E., Müller, C. W., & Diederichs, K. (1990) *J. Mol. Biol. 213*, 627−630.
Swindells, M. B., Orengo, C. A., Jones, J. T., Pearl, L. H., & Thornton, J. M. (1993) *Nature 362*, 299.
Tepper, A. D., Dammann, H., Bominaar, A. A., & Véron, M. (1994) *J. Biol. Chem. 269*, 32175−32180.
Timmons, L., Hersperger, E., Woodhouse, E., Xu, J., Liu, L. Z., & Shearn, A. (1993) *Dev. Biol. 158*, 2.
van Nuland, N. A. J., Boelens, R., Scheek, R. M., & Robillard, G. T. (1995) *J. Biol. Mol. 246*, 180−193.
Villafranca, J. J., & Nowak, T. (1992) *Enzymes, 3rd Ed. 20,* 63−94.
Wallet, V., Mutzle, R., Troll, H., Barzu, O., Wurster, B., Véron, M., & Lacombe, M. L. (1990) *J. Natl. Cancer Inst. 82*, 1199−1202.
Wei, Y.-F., & Matthews, H. R. (1991) *Methods Enzymol. 200*, 388−414.
Williams, R. L., Oren, D. A., Munoz-Dorado, J., Inouye, S., Inouye, M., & Arnold, E. (1993) *J. Mol. Biol. 234*, 1230−1247.
Wittekind, M. G., Reizer, J., & Klevit, R. E. (1990) *Biochemistry 29*, 7191−7200.
Wolodko, W. T., Fraser, M. E., James, M. N. G., & Bridger, W. A. (1994) *J. Biol. Chem. 269*, 10883−10890.
Worthylake, D., Meadow, N. D., Roseman, S., Liao, D. I., Herzberg, O., & Remington, S. J. (1991) *Proc. Natl. Acad. Sci. USA 88*, 10382−10386.

BI9506233